# Numerical Simulation of Wind Tunnel Wall Effects on the Transonic Flow around an Airfoil Model

K. Richter and H. Rosemann

**Abstract.** For wind tunnel measurements in closed-wall test sections, possible interference effects of the wind tunnel walls play an important role. Three-dimensional TAU simulations were performed for the transonic flow around an airfoil model in the adaptive-wall test section of the Transonic Wind Tunnel Göttingen (DNW-TWG) to investigate the existence of wind tunnel wall effects. The results revealed a global side wall interference that is affecting the entire flow around the model and a local side wall interference disturbing the flow in the supersonic regime.

## 1 Introduction

The quality of the flow within the test section is of essential importance for the quality of the entire wind tunnel experiment. In addition to the significance of the basic flow characteristics, such as low turbulence, parallel flow alignment and constant free stream conditions, possible interference effects of the wind tunnel walls play an important role especially for measurements in closed-wall test sections. 'Adaptive-wall test sections' aim to minimize the interference effects of upper and lower walls by adaptation of the wall shape to the prevailing flow condition. Since the side walls usually remain fixed, adaptive-wall test sections are particularly suitable for the investigation of two-dimensional airfoil models.

At the DLR, two-dimensional airfoil measurements in the Transonic Wind Tunnel Göttingen (DNW-TWG) are typically performed in the adaptive-wall test section. In the past, several measurements were conducted with the transonic airfoil model 'VC-Opt' to investigate the effect of flow control devices on an airfoil at transonic speeds. VC-Opt is a turbulent supercritical airfoil designed for the outboard wing region of modern transport aircraft and the model was built in the frame of the DLR project "Adaptive Wing" (ADIF) in 1998. The results measured with

K. Richter · H. Rosemann
DLR, AS-HE, Bunsenstr. 10, 37073 Göttingen, Germany
e-mail: {kai.richter,henning.rosemann}@dlr.de

A. Dillmann et al. (Eds.): *New Results in Numer. & Exp. Fluid Mech.*, NNFM 121, pp. 525–532.
DOI: 10.1007/978-3-642-35680-3_62 

this model have normally been of good quality but some results showed an unexpected behavior that could not be explained by simple two-dimensional flow assumptions. On the one hand, the agreement of the lift curves of experimental results and standard two-dimensional CFD results obtained with MSES or DLR-TAU was not satisfying. The measured lift curve had a lower slope $\mathrm{d}c_l/\mathrm{d}\alpha$ than the numerical result, leading to a difference in the angle of attack at constant lift of up to $\alpha = 0.8°$, shown in fig. 1 (left) for $M = 0.755$. On the other hand, the measured drag polars revealed an unexpected drag rise behavior at high Mach numbers, shown in fig. 1 (right). For a Mach number of $M = 0.790$, drag decreases at lift coefficients above $c_l \approx 0.7$ changing the drag rise characteristics compared to those known for turbulent airfoils.

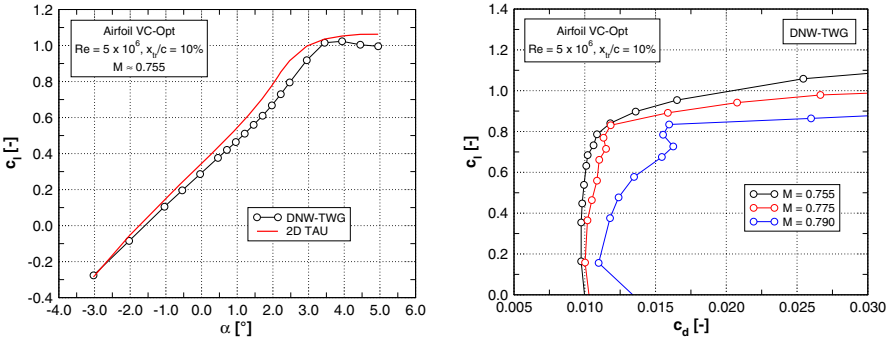


**Fig. 1** Measured and numerical lift curves for the VC-Opt airfoil at $Re = 5 \times 10^6$ and $M \approx 0.755$ (left), and measured drag polars at $Re = 5 \times 10^6$ and $M \in [0.755, 0.775, 0.790]$ (right)

Conventional two-dimensional approaches were not successful to explain or correct these phenomena. Investigations with respect to the influences of the usual experimental and numerical parameters, such as freestream offsets $\Delta M$, $\Delta Re$, $\Delta\alpha$, airfoil deformation, boundary layer transition, computational grid and turbulence models, showed that they all have an effect much smaller than necessary to explain the discrepancies. Because of this, the two-dimensionality of the flow about the airfoil was questioned and wind tunnel wall effects were suspected of playing a role. In order to investigate the existence of wall effects and to study the three-dimensionality of the flow around the model, three-dimensional TAU simulations of the VC-Opt model in the DNW-TWG adaptive-wall test section were conducted and the results are discussed in this paper.

## 2 Experimental Setup and Numerical Tools

### *2.1 Wind Tunnel Experiments*

The experimental data used in this work was measured with the two-dimensional airfoil model VC-Opt in the Transonic Wind Tunnel Göttingen (DNW-TWG) [4] at a

Reynolds number of $Re = 5 \times 10^6$, Mach numbers of $0.755 \leq M \leq 0.790$ and angles of attack of $-3^\circ \leq \alpha \leq 5^\circ$. The 1 m × 1 m adaptive-wall test section was used. Wall adaptation was performed for each test point based on the two-dimensional Cauchy-method by Amecke [2] using the measured top and bottom wall pressure distributions. Remaining interference effects of the upper and lower walls still present at the model position after the adaptation were taken into account in the form of corrections to the freestream dynamic pressure and model angle of attack. For the measurements performed, those were mainly in the order of $\Delta M = 0.005$ and $\Delta\alpha = -0.06^\circ$.

The VC-Opt airfoil model had a chord of $l = 0.4\,\text{m}$ and a span of $b = 1.18\,\text{m}$ (model goes through the side walls) and was equipped with 154 pressure taps for steady pressure measurements. Figure 2 shows a schematic of the airfoil and a photograph of the model installed in the DNW-TWG. Transition was tripped at $x_{tr}/l = 10\%$ with a transition strip on both model sides. Lift, drag and pitching moment coefficients were computed from the steady pressures meausured on the model surface and in the wake. The model was positioned with an accuracy in the angle of attack of $\Delta\alpha = 0.02^\circ$ and the repeatability of a test point with respect to lift and drag coefficients was $\Delta c_l = 0.005$ and $\Delta c_d = 0.0002$ for test points with attached flow. Further details of the experiments are given in [11].

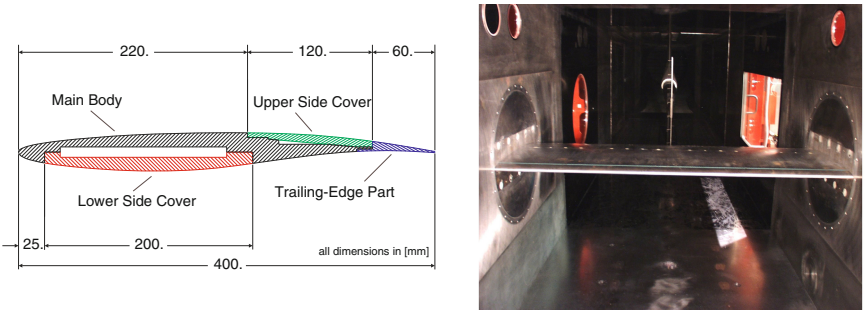


**Fig. 2** Schematic of the VC-Opt airfoil model (left) and photograph of the model installed in the DNW-TWG adaptive-wall test section (right)

## 2.2 DLR-TAU Simulations

Three-dimensional steady RANS simulations were performed with the DLR-TAU code [9] on hybrid grids generated with the commercial grid generation software CENTAUR [1]. The grids represented a symmetric half of the DNW-TWG adaptive-wall test section ($l_{AW} = 4.51\,\text{m}$) with curved upper and lower walls using the adapted wall shapes measured in the experiment. A straight inlet extension ($l_{IE} = 2.6\,\text{m}$) was used in addition to adjust the side wall boundary layer characteristics to measured values [10], as shown in fig. 3. Both the wind tunnel walls and the model surfaces were treated as viscous walls with 30 prismatic layers, the height of the first layer was adjusted to $y^+ \approx 1$ and the height of the prism stack was adjusted to the respective boundary layer thickness. The inflow boundary condition was given with the

total pressure $p_0$ and the total density $\rho_0$ from the experiments, the pressure at the exit plane $p_{exit}$ was adjusted to reach the correct free stream pressure $p_\infty$ in the test section. In the wind tunnel center section a symmetry plane was used.

Two sets of grids were generated. For the simulation of the global side wall interference effect, section 3.1, the airfoil model was resolved with approx. 400 grid points in chordwise and 150 points in spanwise direction. The intersection region of model and side wall had a maximum cell size of 2 mm. Wind tunnel walls were resolved with cell sizes of a maximum of 30 mm. For the simulation of the local side wall interference effect, section 3.2, the grid resolution was increased in large portions of model and side wall to a maximum cell size of 1 mm. The sizes of the grids varied between $4 \times 10^6$ and $9 \times 10^6$ points.

As the simulations aimed to reveal possible side wall effects in the experiment rather than to predict them quantitatively, only a limited grid convergence study was undertaken and is not shown here. All computations were performed with the Spalart-Allmaras turbulence model with modifications according to Edwards [6].

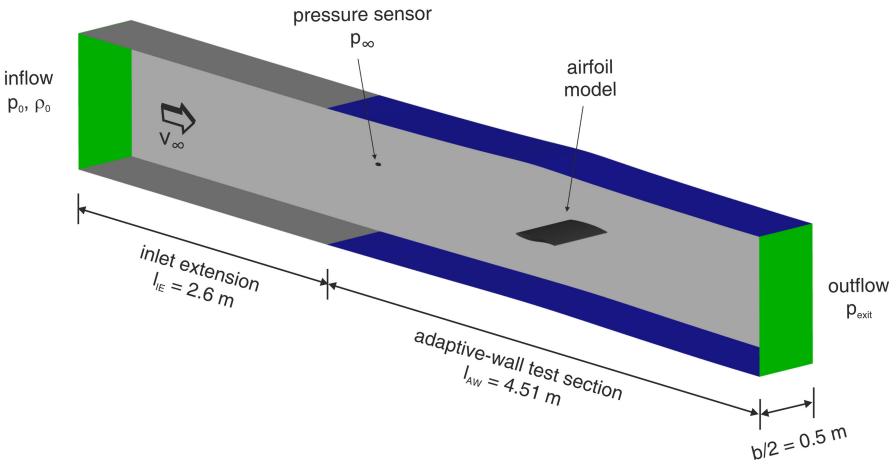


**Fig. 3** Numerical setup of the VC-Opt airfoil model in the DNW-TWG adaptive-wall test section used for 3D TAU simulations

## 3 Results

The numerical simulations of the VC-Opt airfoil model in the DNW-TWG adaptive-wall test section revealed two kinds of side wall interferences affecting the airfoil flow and the measured results. A global side wall interference is affecting the entire flow around the model and a local side wall interference is affecting the flow within the supersonic region on the airfoil upper side.

### *3.1 Global Side Wall Interference Effect*

Comparing the pressure distributions of experiment and two-dimensional numerical simulation for constant angles of attack, the measured distributions persistently show higher suction peak pressures than the 2D CFD data, depicted in fig. 4 for $M \approx 0.755$, $\alpha \approx 0.5^\circ$ and $\alpha \approx 2^\circ$. Nevertheless, for shock-free airfoil flow at $\alpha \approx 0.5^\circ$, the agreement of the pressure distributions is fair and the discrepancy in lift is rather small, compare fig. 1 (left). For airfoil flows with shocks however, an additional upstream movement of the shock can be seen, leading to a reduction in the length of the supersonic flow field and therefore leading to a large difference in lift. These two factors were found to cause the change in the lift slope between the measured results and the 2D CFD predictions.

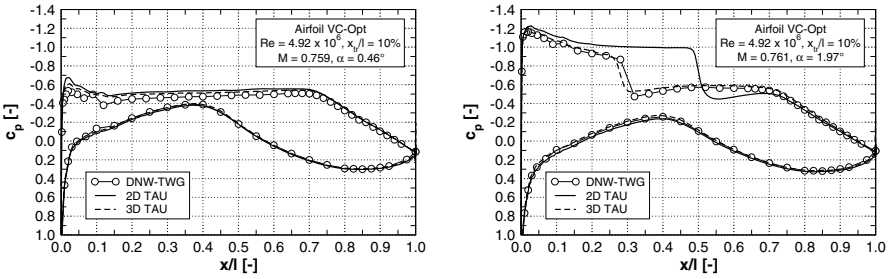


**Fig. 4** Measured and numerical pressure distributions of the VC-Opt airfoil at $Re = 5 \times 10^6$, $M \approx 0.755$ and $\alpha \approx 0.5^\circ$ (left) as well as $\alpha \approx 2^\circ$ (right)

The 3D TAU simulations with wind tunnel walls indicate that the presence of the walls causes the different behavior of suction peak and shock. Figure 4 also shows the numerical center line pressure distributions of the model in the wind tunnel. For shock free flow, a small influence of the walls can be seen in a slight increase in the suction peak pressure compared to the 2D result and leading to a slight decrease in lift. For flows with shocks, a large interference effect can be observed since the shock moves upstream to the position measured in the experiment. The agreement of the pressure distributions is now as good as for shock-free flows and the predicted lift comes close to the lift measured in the experiment. The 3D TAU results have approximately the same lift slope as the measured data.

This wall influence could be identified as a side wall interference originating from a separation bubble existing on the side wall and the model upper side in the region of the trailing edge. Figure 5 depicts the surface pressure distribution on the model upper surface for $M \approx 0.755$ and $\alpha \approx 2^\circ$, with the wind tunnel side wall at $y/b = 0.0$ and the model center line at $y/b = 0.5$. Both the pressure distribution and the wall shear-stress lines clearly reveal a significant influence of the side wall on the flow around the model, causing three-dimensional flow to a large extent. The existence of the 'corner separation' is known in general but the impact on the flow around the transonic VC-Opt airfoil is much larger than expected. The form of the shock front

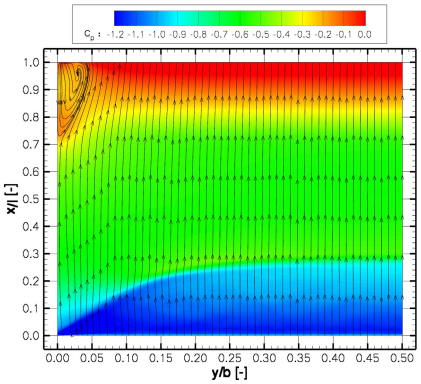


**Fig. 5** Numerical surface pressure distribution and wall shear-stress lines on the upper side of the VC-Opt airfoil at $Re = 5 \times 10^6$, $M \approx 0.755$ and $\alpha \approx 2.0°$ ($y/b = 0.00$ : side wall, $y/b = 0.50$ : center section)

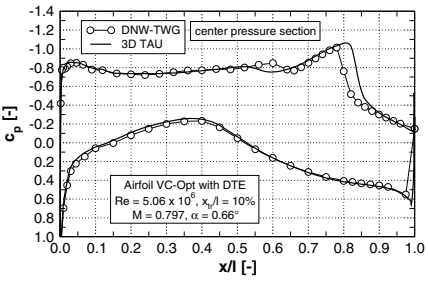


**Fig. 6** Measured and numerical pressure distributions of the VC-Opt airfoil with divergent trailing-edge ($l_{DTE}/l = h_{DTE}/l = 1.0\%$) at $Re = 5 \times 10^6$, $M \approx 0.790$ and $\alpha \approx 0.5°$

in particular is altered, changing from a straight line to a curved shock front. Two-dimensional flow only exists from $y/b \approx 0.40$ but with different 2D conditions in the center of the model than without side walls, as clearly displayed by the pressure distributions in fig. 4. A similar impact of the corner separation on the transonic airfoil flow in the DNW-TWG was also found for an NLR7301 airfoil [7].

## *3.2 Local Side Wall Interference Effect*

The measured pressure distributions of the data points in the unexpected drag rise region in fig. 1 (right) were found to have abnormal 'pressure steps' within the supersonic flow field. These steps exist in all three spanwise pressure sections on the model upper side but at different chordwise locations. Figure 6 presents the center pressure distribution of the VC-Opt airfoil in divergent trailing-edge configuration for $M \approx 0.790$ and $\alpha \approx 0.5°$ as an example, showing the pressure step at $x/l \approx 0.62$. The geometric positions of the disturbances on the model surface suggest a propagation of the disturbance starting from the intersection of the model leading edge with the side wall. The disturbance causes a reduction of the shock strength even into the model center section, leading to both a quantitative and a qualitative change in the drag behavior. Very similar interference effects were observed in 2D airfoil measurements at NLR [5] and ARA [8]. Here, a deformation of the wind tunnel side wall boundary layer was suspected as the cause of the disturbance.

The 3D TAU simulations with wind tunnel walls were able to reproduce the disturbances seen in the experiment. Figure 6 also shows the numerical pressure distribution at the center pressure section of the model. The predicted pressure steps are generally in good qualitative agreement with the measured data. The simulations showed furthermore that the disturbance is a skewed weak shock on the model upper

surface that is generated at the intersection between the model leading edge and the side wall, as depicted in the surface pressure distribution on the model upper side in fig. 7 (left). The shock wave is propagating over the surface and weakens slightly but still reaches into the model center section. The presence of two-dimensional flow is thereby excluded.

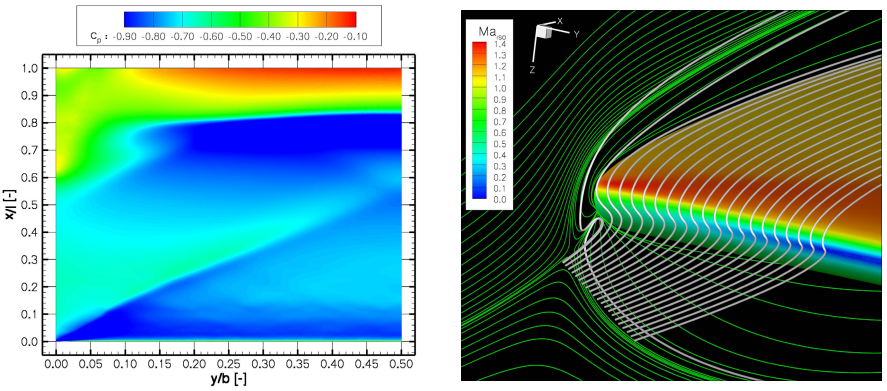


**Fig. 7** Numerical surface pressure distribution (left) and side wall shear-stress lines, streamlines and isentropic Mach number distribution (right) on the upper side of the VC-Opt airfoil with divergent trailing-edge ($l_{DTE}/l = h_{DTE}/l = 1.0\%$) at $Re = 5 \times 10^6$, $M \approx 0.790$ and $\alpha \approx 0.5°$

A simple deformation of the side wall boundary layer was not found to cause the weak shock. Instead, the simulation results show that the shock is generated by the horseshoe vortex occurring at the intersection of model and wall. The existence of a horseshoe vortex in the flow around an obstacle on a flat plate is well known [3, 12]. In the present case, the wind tunnel model represents the obstacle on the wind tunnel side wall. The side wall boundary layer separates upstream of the model leading edge and is displaced to the top and bottom of the model. Figure 7 (right) shows the shear-stress lines (green) on the side wall, the isentropic Mach number distribution on the model surface and streamlines. The wall shear-stress lines indicate the separation line of the recirculation area in which the spiral horseshoe vortex is wrapping around the model. The vortex induces spanwise velocities on the model surface in the direction of the side wall, causing the flow to turn towards the side wall as indicated by the streamlines. This effect is strongest for the near-wall flow and decreases with increasing distance from the side wall. On the way around the leading edge, the flow is accelerated to supersonic speeds just like a normal transonic airfoil flow. In the supersonic field, the skewed flow is then hitting the side wall and is forced to align parallel to the wall. In supersonic flow, this is typically accompanied by a weak shock propagating through the supersonic field, causing the disturbances seen in the experiment that decrease the local Mach number in the supersonic regime. The change in the drag rise characteristics of the VC-Opt airfoil was therefore caused by the presence of the horseshoe vortex.

## 4 Conclusions

Three-dimensional TAU simulations were performed for the transonic flow around the VC-Opt airfoil model in the DNW-TWG adaptive-wall test section to investigate the existence of wind tunnel wall effects. The results revealed two kinds of interference effects. A global side wall interference effect caused by a corner separation on the model upper side was affecting the entire flow around the model and was changing the slope of the lift curve. A local side wall interference effect caused by the horseshoe vortex at the intersection of model and side wall was disturbing the flow in the supersonic regime and was altering the drag characteristics of the model at high free stream Mach numbers.

## References

1. http://www.centaursoft.com
2. Amecke, J.: Direkte Berechnung von Wandinterferenzen und Wandadaption bei zweidimensionaler Strömung in Windkanälen mit geschlossenen Wänden. Forschungsbericht DFVLR FB 1985-62, DFVLR (1985)
3. Baker, C.J.: The turbulent horseshoe vortex. Journal of Wind Engineering and Industrial Aerodynamics 6(1-2), 9–23 (1980)
4. Binder, B., Riethmüller, L., Tusche, S., Wulf, R.: Modernisierung des Transsonischen Windkanals in Göttingen. DGLR Jahrbuch 1, 237–249 (1992)
5. Dambrink, H.A.: Investigation of the 2-dimensionality of the flow around a profile in the NLR $0.55 \times 0.42\ m^2$ transonic wind tunnel. Technical Report NLR AC-72-018, NLR (1972)
6. Edwards, J., Chandra, S.: Comparison of Eddy Viscosity-Transport Turbulence Models for Three-Dimensional, Shock-Separated Flowfields. AIAA Journal 34(4) (1996)
7. Gardner, A.D., Richter, K., Rosemann, H.: Prediction of the Wind Tunnel Sidewall Effect for the iGREEN Wing-Tailplane Interference Experiment. In: Dillmann, A., Heller, G., Klaas, M., Kreplin, H.-P., Nitsche, W., Schröder, W. (eds.) New Results in Numerical and Experimental Fluid Mechanics VII. NNFM, vol. 112, pp. 75–82. Springer, Heidelberg (2010)
8. GARTEur Action Group AD (AG-02): Two-Dimensional Transonic Testing Methods, Final Report. Technical Report NLR TR 83086 U, NLR (1981)
9. Gerhold, T., Friedrich, O., Evans, J., Galle, M.: Calculation of Complex Three-Dimensional Configurations Employing the DLR-TAU-Code. In: AIAA-97-0167, AIAA 35th Aerospace Sciences Meeting and Exhibit, Reno (NV) (1997)
10. Potin, O.: Grenzschichtermittlung im Transsonischen Windkanal Göttingen (TWG). Interner Bericht 29112-1996 B 02, DLR (1996)
11. Richter, K., Rosemann, H.: Experimental investigation of trailing-edge devices at transonic speeds. The Aeronautical Journal 106(1058), 185–193 (2002)
12. Sieverding, C.H.: Recent progress in the understanding of the basic aspects of secondary flows in turbine blade passages. Journal of Engineering for Gas Turbines and Power 107(2), 248–257 (1985)